

1 **Attenuated metabolism is a hallmark of obesity as revealed by**  
2 **comparative proteomic analysis of human omental adipose tissue**

3

4 Rafael Pérez-Pérez<sup>a,b</sup>, Eva García-Santos<sup>a,b</sup>, Francisco J. Ortega-Delgado<sup>b,c</sup>, Juan A. López<sup>d</sup>,  
5 Emilio Camafeita<sup>d</sup>, Wifredo Ricart<sup>b,c</sup>, José-Manuel Fernández-Real<sup>b,c</sup>, Belén Peral<sup>a,b,\*</sup>

6

7 <sup>a</sup>Instituto de Investigaciones Biomédicas, Alberto Sols, Consejo Superior de Investigaciones  
8 Científicas (CSIC) & Universidad Autónoma de Madrid, E-28029 Madrid, Spain

9 <sup>b</sup>CIBER Fisiopatología de la Obesidad y Nutrición (CIBEROBN) ISCIII, Spain

10 <sup>c</sup>Department of Diabetes, Endocrinology and Nutrition, Hospital Dr. Josep Trueta, E-17007

11 Girona, Spain

12 <sup>d</sup>Unidad de Proteómica, Centro Nacional de Investigaciones Cardiovasculares (CNIC), E-28029  
13 Madrid, Spain

14

15 \*Corresponding author: Instituto de Investigaciones Biomédicas, Alberto Sols, Consejo  
16 Superior de Investigaciones Científicas (CSIC) & Universidad Autónoma de Madrid, Arturo

17 Duperier 4, E-28029 Madrid, Spain. Tel: 34-915854478. Fax: 34-915854401. E-mail:

18 bperal@iib.uam.es

19

20 ABSTRACT

21 Obesity is recognized as an epidemic health problem worldwide. In humans, the accumulation  
22 of omental rather than subcutaneous fat appears to be tightly linked to insulin resistance, type 2  
23 diabetes and cardiovascular disease. Differences in gene expression profiles in the adipose  
24 tissue comparing non-obese and obese subjects have been well documented. However, to date,  
25 no comparative proteomic studies based on omental fat have investigated the influence of  
26 obesity in protein expression. In this work, we searched for proteins differentially expressed in  
27 the omental fat of non-obese and obese subjects using 2D-DIGE and MS. Forty-four proteins,  
28 several of which were further studied by immunoblotting and immunostaining analyses, showed  
29 significant differences in the expression levels in the two groups of subjects. Our findings reveal  
30 a clearly distinctive proteomic profile between obese and non-obese subjects which emphasizes:  
31 i) reduced metabolic activity in the obese fat, since most down-regulated proteins were engaged  
32 in metabolic pathways; and ii) morphological and structural cell changes in the obese fat, as  
33 revealed by the functions exerted by most up-regulated proteins. Interestingly, transketolase and  
34 aminoacylase-1 represent newly described molecules involved in the pathophysiology of  
35 obesity, thus opening up new possibilities in the study of obesity.

36

37

38 Keywords: 2D-DIGE, MALDI-MS, obesity, human adipose tissue, omental fat, TKT, ACY-1,  
39 comparative proteomic study, metabolic pathways

40

## 41 **1. Introduction**

42

43 Obesity is one of the most important public health problems facing the world today and has  
44 increased dramatically over the last decades in children and adolescents [1]. Obese subjects  
45 suffer from decreased life quality and expectancy as well as increased risk of suffering insulin  
46 resistance, type 2 diabetes, cardiovascular disease (CVD), hepatic steatosis, pulmonary and  
47 muscular pathologies, psychological disorders and cancer, among others [2]. A person's weight  
48 and body composition are likely determined by interaction between his/her genetic makeup and  
49 social, cultural, behavioral, and environmental factors. The intake of energy-dense foods,  
50 especially when combined with reduced physical activity, is very likely to contribute to the high  
51 prevalence of obesity; however, the existence of complex systems that regulate energy balance  
52 calls for a broader view of this paradigm [3].

53 In humans, the adipose tissue is dispersed throughout the body with major intra-abdominal  
54 depots around the omentum, intestines, and perirenal areas, as well as in subcutaneous depots in  
55 the buttocks, thighs, and abdomen. These two fat depots, the subcutaneous and the omental fat,  
56 exhibit unique biochemical and cellular properties, such as response to sex hormones, and  
57 different secretion profiles [4], including a different lipolytic program [5]. Moreover, the  
58 omental, but not the subcutaneous, fat drains directly into the portal circulation, and some data  
59 point out to excessive free fatty acid release from the omental adipose tissue in central obesity  
60 [6]. In fact, it is well established that the size of the omental, more than the subcutaneous, fat is  
61 strongly related to a higher risk of obesity-related co-morbidities, including insulin resistance,  
62 type 2 diabetes, dyslipidemia and CVD. As a consequence of extensive recent investigation, the  
63 adipose tissue is no longer regarded a mere fat reservoir, but an endocrine organ which cross-  
64 talks with other essential organs like the liver, the muscle, the pancreas, and the brain, being a  
65 crucial regulator of whole-body homeostasis.

66 Gene expression studies (i.e. microarrays and RT-PCR) using adipose tissue from obese and  
67 non-obese subjects have yielded important insights into the pathogenesis of obesity and related  
68 diseases, (reviewed in [7]). Results pointed out that: i) obesity represents a chronic

69 inflammatory condition, since genes related with inflammation are up-regulated in response to  
70 obesity; ii) the differentiation state of obese adipocytes is altered; and iii) the expression of  
71 adipogenic genes is decreased in obesity [8-11]. As far as the latter is concerned, it has been  
72 suggested that the limited lipogenic and/or adipogenic capacity of obese adipocytes might lead  
73 to spillover of excess lipids to other tissues, and lipotoxicity could contribute to the  
74 pathogenesis of type 2 diabetes [12].

75 At the protein level the knowledge about human adipose tissue is limited. A very few proteomic  
76 studies have been published using either whole adipose tissue or isolated cells from both fat  
77 depots (reviewed in [13]). The majority of these works have studied human adipogenesis or  
78 adipose tissue secretome. Recently, however, our group and others have resorted to 2D-DIGE  
79 and MS to explore the differences between omental and subcutaneous fat [14-16]. Despite of  
80 some drawbacks inherent to 2-DE analysis (mainly the poor representation of low-abundant or  
81 very hydrophobic proteins as well as those with extreme pI and molecular weight), the  
82 quantitative comparison of proteins in two or more conditions based on 2D-DIGE/MS is a  
83 widespread, robust methodology to assess differential protein expression. This approach  
84 provides great analytical precision, dynamic range and sensitivity, therefore allowing a  
85 reproducible and reliable differential analysis [17]. Nevertheless, to date, no proteomic studies  
86 based on omental fat have investigated the influence of obesity in protein expression, given that  
87 the omental adipose tissue has been tightly linked to obesity-associated co-morbidities. In this  
88 work, we have compared for the first time the omental fat from non-obese and morbidly obese  
89 subjects by 2D-DIGE and MS, revealing 44 modulated proteins in response to obesity. Our  
90 findings emphasize a noticeably decreased expression of proteins related to metabolic processes  
91 in response to obesity together with a down-regulation of mitochondrial enzymes, which is  
92 consistent with a reduced metabolic activity in the obese adipose tissue. In addition, most of the  
93 proteins found up-regulated in obesity develop structural functions in the cell, which account for  
94 the morphological changes undergone by obese adipocytes. Therefore, our results support a  
95 neatly distinctive biological profile in the omental fat of obese and non-obese subjects regarding  
96 protein expression.

97 **2. Materials and methods**

98

99 2.1. Study design

100 Omental fat from morbidly obese ( $n=6$ ) and non-obese ( $n=6$ ) subjects obtained during surgery  
101 were analyzed by a proteomic approach using 2D-DIGE. Samples were labelled using  
102 fluorophore dye-swapping to avoid labelling bias, combined in pairs and separated by  
103 electrophoresis. Image analysis revealed modulated proteins which were identified by MS.  
104 Results validation was performed by Western Blot with an additional set of subjects.  
105 Immunostaining assays were performed to study selected proteins not only in adipose tissue  
106 samples, but also in human omental adipocyte cultures. The 3T3-L1 cell line was used to study  
107 whether these proteins were modulated in the adipocyte differentiation process.

108

109 2.2. Biological samples

110 Omental adipose tissue samples were obtained from 26 women, including 12 non-obese and 14  
111 morbidly obese. Non-obese subjects had a body mass index (BMI)  $< 30 \text{ kg/m}^2$  (BMI ranged  
112 from 22.1 to 28.3  $\text{Kg/m}^2$ ), and age ranged from 25 to 56 years. Morbidly obese subjects had a  
113 BMI  $> 40 \text{ kg/m}^2$  (BMI ranged from 40.7 to 48.5  $\text{Kg/m}^2$ ), and age ranged from 39 to 58 years.  
114 All these subjects had been submitted for elective surgical procedures (cholecystectomy,  
115 surgery of abdominal hernia and gastric by-pass surgery). During surgery, biopsies of adipose  
116 tissues were obtained after an overnight fast, washed in chilled 9 g/L NaCl solution, partitioned  
117 into pieces, and immediately frozen in liquid nitrogen and stored at  $-80^\circ\text{C}$  until protein  
118 extraction. The surgeon aimed to obtain the samples from similar anatomical locations in all the  
119 subjects. All women were of Caucasian origin and reported that their body weight had been  
120 stable for at least three months before the study. None of the subjects had type 2 diabetes or any  
121 other systemic disease apart from obesity and all were free of any infections within the previous  
122 month before the study. Liver disease and thyroid dysfunction were specifically excluded by  
123 biochemical work-up. Other exclusion criteria for those patients included the following: 1)  
124 clinically significant hepatic, neurological, or other major systemic disease, including

125 malignancy; 2) history of drug or alcohol abuse, defined as >80 g/day, or serum transaminase  
126 activity more than twice the upper normal range limit; 3) elevated serum creatinine  
127 concentrations; 4) acute major cardiovascular event in the previous 6 months; 5) acute illnesses  
128 and current evidence of chronic inflammatory or infectious diseases; and 6) mental illness  
129 rendering the subjects unable to understand the nature, scope, and possible consequences of the  
130 analysis. The study was conducted according to the recommendations of the Declaration of  
131 Helsinki and was approved by the ethics committees of Hospital Dr. Josep Trueta (Girona,  
132 Spain). Signed informed consent was obtained from all subjects.

133

### 134 2.3. 2D-DIGE analysis

135 Proteins were extracted from omental adipose tissue biopsies (100 mg) by using the 2D  
136 Grinding Kit (GE Healthcare, Uppsala, Sweden) in Lysis Buffer (7 M urea, 2 M thiourea, 4%  
137 CHAPS, and 30 mM Tris-HCl pH 8.5) containing 50 mM DTT. The extract was shaken for 30  
138 min at room temperature and centrifuged at 15000xg for 30 minutes. Proteins were precipitated  
139 with the 2D-CleanUp Kit (GE Healthcare) and redissolved in Lysis Buffer. The protein  
140 concentration was determined using RC/DC Protein Assay (Bio-Rad Laboratories, Hercules,  
141 CA, USA). Proteins were labelled according to the manufacturer's instruction (GE Healthcare).  
142 Briefly, 50 µg of adipose tissue protein extracts were minimally labeled with 400 pmol of the *N*-  
143 hydroxysuccinimide esters of Cy3 or Cy5 fluorescent cyanine dyes on ice in the dark for 30 min.  
144 All experiments comprised an internal standard containing equal amounts of each cell lysate,  
145 which was labelled with Cy2 dye. The labelling reaction was quenched with 1 µl of 10 mM  
146 lysine on ice in the dark for 10 min. The internal standard and the individual omental fat extracts  
147 from non-obese and obese subjects were combined and run in a single gel (150 µg total  
148 proteins). Proteins extracts were diluted in Rehydration Buffer (7 M urea, 2 M thiourea, 2%  
149 CHAPS, 0.8% (v/v) IPG buffer 3-11NL), reduced with 50 mM DTT, and applied by cup-  
150 loading to 24 cm IPG strips pH 3-11NL, which were previously rehydrated with Rehydration  
151 Buffer containing 100 mM hydroxyethyl disulfide (DeStreak, GE Healthcare). The first and

152 second dimension together with the equilibration step were performed following the procedure  
153 previously described [14].

154

#### 155 2.4. Image acquisition and analysis

156 After SDS-PAGE, gels were scanned with a Typhoon 4100 scanner (GE Healthcare) at 100  $\mu$ m  
157 resolution using appropriate individual excitation and emission wavelengths, filters and  
158 photomultiplier (PMT) sensitivity for each Cy2, Cy3 and Cy5 dyes (PMT values: 510, 510 and  
159 475 respectively). Gel images were analyzed with the DIA (Differential in-gel Analysis) module  
160 of the DeCyder v7 software (GE Healthcare) for automatic spot detection, background  
161 subtraction, quantification and normalization with low experimental variation (DeCyder  
162 Differential Analysis Software User Manual, version 7; GE Healthcare, 2009). The Biological  
163 Variation Analysis (BVA) module utilized those images individually processed with the DIA  
164 module to match protein spots across gels, using the internal standard for gel-to-gel matching.  
165 Statistical analysis was then carried out to determine protein expression changes. P values lower  
166 than 0.05 as calculated from Student's t test were considered significant. Multivariate analysis  
167 was performed by Principal Components Analysis (PCA) using the algorithm included in the  
168 Extended Data Analysis (EDA) module of the DeCyder software based on the spots matched  
169 across all gels.

170

#### 171 2.5. In-gel trypsin digestion and mass spectrometry

172 Protein spots showing significantly altered expression levels in the 2 groups of samples by  
173 DeCyder Software were selected for gel excision from silver-stained gels, digested  
174 automatically on a Proteineer DP robot (Bruker Daltonik, Bremen, Germany) using the protocol  
175 of [18] and analyzed in an Ultraflex MALDI TOF/TOF mass spectrometer (Bruker Daltonik)  
176 [19] to obtain the corresponding MALDI-MS and MALDI-MS/MS spectra. In a first step,  
177 MALDI-MS spectra were acquired by averaging 300 individual spectra in the positive ion  
178 reflector mode at 50 Hz laser frequency in a mass range from 800 to 4000 Da. In a second step,  
179 precursor ions showing in the MALDI-MS mass spectrum were subjected to fragment ion

180 analysis in the tandem (MS/MS) mode to average 1000 spectra. Peak labelling, internal  
181 calibration based on two trypsin autolysis ions with  $m/z = 842.510$  and  $m/z = 2211.105$ , as well  
182 as removal of known trypsin and keratin peptide masses were performed automatically using the  
183 flexAnalysis 2.2 software (Bruker Daltonik). No smoothing or any further spectral processing  
184 was applied. MALDI-MS and MS/MS spectra were manually inspected in detail and reacquired,  
185 recalibrated and/or relabelled using the aforementioned programs and homemade software when  
186 necessary.

187

## 188 2.6. Database searching

189 MALDI-MS and MS/MS data were combined through the BioTools 3.0 program (Bruker  
190 Daltonik) to search a nonredundant protein database (NCBI nr 20091022;  $\sim 7.0 \times 10^6$  entries;  
191 National Centre for Biotechnology Information, Bethesda, USA), using the Mascot 2.2 software  
192 (Matrix Science, London, UK; <http://www.matrixscience.com>) [20]. Other relevant search  
193 parameters were set as follows: enzyme, trypsin; fixed modifications, carbamidomethyl (C);  
194 allow up to 1 missed cleavage; peptide tolerance  $\pm 20$  ppm; MS/MS tolerance  $\pm 0.5$  Da. Protein  
195 scores greater than 81 were considered significant ( $p < 0.05$ ).

196

## 197 2.7. Cell culture and adipocyte differentiation

198 Isolated human omental pre-adipocytes (Zen-Bio, Inc. Raleigh, NC, USA) were cultured with  
199 omental pre-adipocytes medium (Zen-Bio, Inc.) at  $37^\circ\text{C}$  and 5%  $\text{CO}_2$  and differentiated using  
200 omental differentiation medium (Zen-Bio, Inc.) according to the method outlined by Ortega et al  
201 [21]. Two weeks after the initiation of differentiation, cells appeared rounded with large lipid  
202 droplets in the cytoplasm and were considered mature adipocytes. Murine 3T3-L1 fibroblasts  
203 (CCL 92.1, American Type Culture Collection) were grown to confluence in DMEM containing  
204 10% calf serum. The differentiation to adipocytes was induced according to the procedure  
205 described by Ortega et al [21]. On days 0, 3, 5 and 9, three replicated cell samples were  
206 separately collected for later immunoassays.

207



## 208 2.8. Immunoblotting analysis

209 Fat tissue or cultured cells were homogenized in radioimmuno precipitation assay (RIPA)  
210 buffer as described in [14]. Protein extracts (*ca.* 10 µg) were loaded, resolved on SDS-PAGE  
211 and transferred to Hybond ECL nitrocellulose membranes by conventional procedures.  
212 Membranes were stained with 0.15% Ponceau red (Sigma-Aldrich, St Louis, MO, USA) to  
213 ensure equal loading after transfer and then blocked with 5% (w/v) BSA or dried nonfat milk in  
214 TBS buffer with 0.1% Tween 20. The antibodies used for Western Blot analysis revealed in  
215 each case single bands at the expected molecular masses. The primary antibodies used were:  
216 1:2000 rabbit anti-TKT (HPA029480), and 1:2000 rabbit anti-ACY-1 (A6609) (Sigma-  
217 Aldrich); 1:2000 goat anti-Beta-actin (sc-1616); 1:4000 rabbit anti-SPHK1 (sc-48825), and  
218 1:200 goat anti-FABP5 (sc-16060) (Santa Cruz Biotechnology); 1:1000 mouse anti-HSP70  
219 (C92F3A-5) (Stressgen Bioreagents); 1:500 rabbit anti-FABP4 (Eurogentec, Seraing, Belgium).  
220 Blots were incubated with the appropriate IgG-HRP-conjugated secondary antibody.  
221 Immunoreactive bands were visualized with ECL-plus reagent kit (GE Healthcare). Blots were  
222 exposed for different times; exposures in the linear range of signal were selected for  
223 densitometric evaluation. Optical densities of the immunoreactive bands were measured using  
224 Image J analysis software. Statistical comparisons of the densitometry data were carried out  
225 using the Student's *t* test for samples, and results were expressed as means ± standard deviation  
226 (SD) using SPSS 16.0 (SPSS Inc., Illinois, USA). Statistical significance was set at  $p < 0.05$ .

227

## 228 2.9. Immunohistochemistry

229 Five-micron sections of formalin-fixed paraffin-embedded adipose tissue were deparaffinised  
230 and rehydrated prior to antigen unmasking by boiling in 1 mM EDTA, pH 8. Sections were  
231 blocked in normal serum and incubated overnight with rabbit anti-TKT (1:500 dilution) or  
232 rabbit anti-ACY-1 (1:200 dilution) antibodies. Secondary antibody staining was performed  
233 using the VECTASTAIN ABC kit (Vector Laboratories, Inc. Burlingame, CA) and detected  
234 with diaminobenzidine (DAB, Vector Laboratories, Inc.). Sections were counterstained with  
235 hematoxylin prior to dehydration and coverslip placement, and examined under a Nikon Eclipse

236 90i microscope. As a negative control, the procedure was performed in the absence of primary  
237 antibody.

238

### 239 2.10. Immunofluorescence

240 Frozen adipose tissue sections or cultured cells were fixed with 4% paraformaldehyde and  
241 permeabilized for 30 min with 0.1% Triton X-100 in PBS. Staining was performed overnight at  
242 4°C with rabbit anti-TKT (1:500 dilution) or with rabbit anti-ACY-1 (1:400 dilution) antibodies,  
243 washed, and visualized using Alexa Fluor 546 goat anti-rabbit antibody (1:500; Molecular  
244 Probes Inc., OR, USA). The slides were counterstained with DAPI (4,6-diamidino-2-  
245 phenylindole) to reveal nuclei. The lipophilic fluorescence dye BODIPY 493/503 was used for  
246 lipid droplet labelling according to the manufacturer's instruction (Molecular Probes Inc.). The  
247 slides were examined under a Leica TCS SP5 fluorescent microscope (Heidelberg, Germany).  
248 As a negative control, the assay was performed in the absence of primary antibody.

249

## 250 **3. Results**

251

### 252 3.1. Proteomic analysis of obese and non-obese adipose tissue samples

253 To detect proteins differentially expressed in obesity, omental fat samples from morbidly obese  
254 ( $n=6$ ) and non-obese ( $n=6$ ) females were analyzed by 2D-DIGE. Protein extracts were labelled  
255 using dye-swapping with either Cy3 or Cy5 fluorescent dye to avoid labelling bias arising from  
256 the fluorescence properties of gels at different wavelengths. Then each Cy3/Cy5-labelled  
257 sample pair was mixed with a Cy2-labelled internal standard and loaded onto each gel. After 2-  
258 DE, the Cy2, Cy3 and Cy5 channels were individually imaged from each gel (Supplemental Fig.  
259 1). Automated image analysis performed with DeCyder software detected approximately 2700  
260 spots per gel in the 3-11 NL pH range with a molecular mass of 10-150 kDa, of which 1200  
261 spots were matched throughout all gels. Multivariate PCA showed that the "non-obese group"  
262 was efficiently discriminated from the "obese group" (data not shown). DeCyder statistical  
263 analyses showed that 70 protein spots were differentially expressed at  $p<0.05$  considering only

264 those spots present in all gels. These spots were excised from silver-stained gels, digested with  
265 trypsin, and analyzed by MALDI-MS followed by database search. Fifty-six spots, which  
266 corresponded to 44 unique proteins could be identified (Fig. 1 and Table 1). Twenty proteins  
267 were increased and 24 decreased in response to obesity.

268

### 269 3.2. Functional classification of the proteins differentially expressed

270 To understand the biological relevance of protein expression changes in response to obesity, the  
271 Protein Analysis Through Evolutionary Relationship (PANTHER) application  
272 (<http://www.pantherdb.org/>) was used. This classification system uses information on protein  
273 sequence to assign a gene to an ontology group on the basis of the Gene Ontology (GO) terms  
274 <http://www.geneontology.org/>. Thus, the two sets of up- and down-regulated proteins were  
275 searched for significantly over-represented ( $p < 0.05$ ) GO terms. Two key Biological Process  
276 classes were found significantly enriched in the group of down-regulated proteins: *Metabolic*  
277 *Process* and *Generation of Precursor Metabolites and Energy*, while three key Biological  
278 Process classes (*Cellular Process*, *Developmental Process* and *Cellular Component*  
279 *Organization*) were significantly enriched in the set of up-regulated proteins. Likewise, the  
280 categorization based on the Molecular Function GO category showed that most down-regulated  
281 proteins accounted for one key significant class, *Catalytic Activity*, while *Structural Molecule*  
282 *Activity* revealed as the unique key GO term with significant enrichment in the up-regulated  
283 proteins from obese adipose tissue (Fig. 2).

284 In addition, PANTHER application mapped the 44 differentially expressed proteins into parent  
285 and child categories with regard to their Molecular Function and Biological Process GO terms  
286 (Supplementary Table 2), highlighting that most of the down-regulated proteins were engaged  
287 in metabolic pathways. Our results have also revealed that the set of down-regulated proteins  
288 comprised numerous (14 out of 24, 58%) mitochondrial enzymes, overall supporting a reduced  
289 metabolic activity in the obese adipose tissue.

290

### 291 3.3. Validation of differential protein expression

292 **Western Blot** analyses were performed in an additional set of non-obese and morbidly obese  
293 women for two proteins whose expression in human adipose tissue had not been previously  
294 documented, TKT and ACY-1, together with two molecules, HSP70 and FABP5 that had been  
295 earlier studied in fat and/or in obesity and related co-morbidities. One of these proteins was  
296 shown up-regulated (HSP70) and the other three were found down-regulated (TKT, ACY-1 and  
297 FABP5) in response to obesity. Immunoblotting analysis using an antibody against TKT  
298 confirmed that this protein was over-expressed ( $p<0.05$ ) in the non-obese group of subjects,  
299 confirming 2-DE findings (Fig. 3). Likewise, ACY-1 levels were significantly more abundant  
300 ( $p<0.05$ ) in the non-obese subjects (Fig. 3), in agreement with 2D-DIGE results. Both TKT and  
301 ACY-1 were studied by immunostaining methods, as well as in the adipocyte differentiation  
302 process. Immunoblotting analysis revealed that HSP70 was significantly increased in obese vs.  
303 non-obese individuals ( $p<0.05$ ), thus confirming 2D-DIGE results (Fig. 3). By using an  
304 antibody anti-FABP5, immunoblotting analysis revealed an over-expression of FABP5 protein  
305 in the omental adipose tissue from non-obese compared to obese subjects; however this result  
306 did not reach statistical significance ( $p=0.06$ ) mostly due to the high SD observed in non-obese  
307 samples (data not shown). It must be noted that **Western Blot** assay may fail to validate  
308 particular protein isoforms found differentially expressed by 2D-DIGE/MS as they rely on  
309 antibodies lacking the necessary specificity.

310

#### 311 3.4. Immunostaining analyses

312 Immunohistochemical and immunofluorescence approaches were performed to determine the  
313 cellular distribution of TKT and ACY-1 proteins in biopsies of omental fat given that, as far as  
314 we know, these proteins have not been earlier analysed in this tissue. TKT was assayed in  
315 sections of omental adipose tissue by both techniques revealing similar results.  
316 Immunofluorescence detection showed a bright staining pattern mainly in the cytoplasm of  
317 adipocytes and of stromal-vascular fraction (SVF) cells, as well as in the nuclei of a few cells  
318 (Fig. 4A). To determine whether the stained nuclei pertained to adipocytes,  
319 immunofluorescence analysis from a cellular culture of human pre-adipocytes and differentiated

320 adipocytes was performed. This analysis showed that in pre-adipocytes TKT was localized in  
321 the cytoplasm as well as in the nucleus, while in adipocytes only the cytoplasm but not the  
322 nucleus was stained (Fig. 4B and 4C). TKT expression was also confirmed in adipose tissue  
323 macrophages by co-staining assays using CD68 (not shown).

324 ACY-1 was also assayed in sections of omental fat by immunostaining analyses, which showed  
325 that ACY-1 was expressed in the cytoplasm as well as in the nucleus of adipocytes and SVF  
326 cells, including omental mesothelial cells (Supplemental Fig. 2A and 2B). Immunofluorescence  
327 analysis revealed the presence of ACY-1 in the nucleus of cultured human omental pre-  
328 adipocytes (Fig. 5A), while in differentiated adipocytes ACY-1 localized around cytosolic lipid  
329 droplets and, to a lesser extent, in the nucleus (Fig. 5B and 5C). In addition, we had also  
330 performed immunofluorescence analysis in 3T3-L1 cells during the adipogenic process. As  
331 illustrated in Supplemental Fig. 3A, ACY-1 was localized exclusively in 3T3-L1 fibroblast  
332 nuclei (day 0), as was the case for human pre-adipocytes; however, in 3T3-L1 differentiated  
333 adipocytes (day 9), ACY-1 was shown around lipid droplets in the cytoplasm, as well as in the  
334 majority of the nuclei (Supplemental Fig. 3B and 3C).

335

### 336 3.5. 3T3-L1 adipogenesis

337 To further study TKT and ACY-1 proteins, we performed immunoblotting analysis with  
338 proteins extracted during the adipogenic maturation of 3T3-L1 cells using the above-described  
339 specific antibodies. TKT and ACY-1 were significantly augmented with adipocyte  
340 differentiation in parallel to the expression of FABP4, which was used as an adipogenesis  
341 control (Fig. 6).

342

## 343 **4. Discussion**

344 Over the last years an increasing number of studies have focused in the analysis of gene  
345 expression to gain insight into obesity and related pathologies. However only a few number of  
346 studies have resorted to proteomic methods to identify human fat proteins associated to these  
347 disorders. In the present study we have employed a proteomic approach based on 2D-DIGE and

348 MALDI-MS to uncover differences in protein expression using biopsies of omental fat from  
349 non-obese and morbidly obese individuals, reporting for the first time a set of 44 proteins that  
350 are significantly modulated in these two sets of subjects. Our study has focused on omental  
351 adipose tissue as this fat depot has been long associated with augmented risk of suffering  
352 pathologies related to obesity [22].

353 The down-regulation of proteins related to metabolic processes such as *Amino Acid Metabolism*,  
354 *Carbohydrate Metabolism* and *Lipid Metabolism* suggests a reduction of metabolic activity in  
355 the obese omental fat, and is consistent with previous mRNA studies [8-10, 23]; thus, Ortega *et*  
356 *al.* [10] demonstrated the down-regulation of the main lipogenic enzymes in obese omental fat  
357 using a large cohort of individuals. In this scenario, these findings provide evidence for an  
358 impaired capacity of the adipose tissue to function as an energy reservoir. In addition, it is  
359 noteworthy the high number of mitochondrial enzymes included in the set of down-regulated  
360 proteins in the obese adipose tissue, 14 proteins out of 24, which is consistent with the reduction  
361 in the oxidative metabolism in obesity. Our findings are in agreement with previous microarray  
362 analysis revealing a coordinated down-regulation of catabolic pathways operating in the  
363 mitochondria such as: fatty acid  $\beta$  oxidation, tricarboxylic acid cycle and electron transport  
364 chain [24]. In addition, a strong correlation between impaired adipocyte mitochondrial activity  
365 and/or content and obesity has been well documented [25-27]. Decreased mitochondrial  
366 capacity in adipocytes may alter adipocyte insulin sensitivity and/or function due to the high  
367 energetic requirements for fatty acid storage, adipokine secretion [28], insulin signalling [29],  
368 and glucose uptake. Therefore, the relatively high number of mitochondrial proteins found  
369 down-regulated in our study is consistent with previous evidences.

370 The set of up-regulated proteins, which pertain to the following significantly enriched classes:  
371 *Cellular Process*, *Developmental Process*, *Cellular Component Organization*, and *Structural*  
372 *Molecule Activity*, suggests that the enlargement of the obese adipocytes, by increasing fat  
373 storage, is accompanied by: i) cytoskeleton changes, such as alteration of LMNA, LMNB1 and  
374 integrin alpha 7; ii) changes in the extracellular matrix (ECM), such as collagen (COL6A3) and  
375 lumican; and iii) tissue structure modifications, such as alteration in epithelial cytokeratins, CK-

376 7, CK-8 and CK-19, compatible with omental mesothelium changes. Our findings showing the  
377 up-regulation of proteins controlling cell architecture and tissue remodelling are in agreement  
378 with previous transcriptomic studies reporting that the expansion of adipose tissue is associated  
379 with a remodelling of ECM together with changes of fat cell cytoskeleton [23, 30] compatible  
380 with the need to adapt fat pads as adiposity increase.

381 Several relevant proteins highlighted by our study were more in-depth analyzed. Transketolase  
382 (TKT) expression levels were reduced in obese patients. To our knowledge this is the first time  
383 that a link between TKT and obesity is reported. This protein is a thiamine diphosphate (ThDP)-  
384 dependent enzyme that catalyzes several reactions in the non-oxidative branch of the Pentose  
385 Phosphate Pathway (PPP). In mammalian cells, the main function of PPP is to produce the  
386 reduced form of nicotinamide-adenine dinucleotide phosphate (NADPH), which functions in  
387 detoxification processes and lipid biosynthesis. Another function of PPP is to convert hexose  
388 into pentose, which is required for nucleic acid synthesis [31]. TKT haploinsufficient mice  
389 showed a markedly reduction in adipose tissue (77%) [32] which could be induced by NADPH  
390 deficiency, limiting the production of lipids in the fat. The reduced levels of TKT found in the  
391 group of obese versus non-obese subjects could be explained by the occurrence of a  
392 compensatory mechanism through which the obese adipose tissue would prevent further  
393 enlargement. In this scenario, during the period of dynamic obesity large amounts of NADPH  
394 are required for fatty acid biosynthesis, and an increase in TKT function is expected. In contrast,  
395 it is well known that lipogenic pathways are reduced in established obesity [10] and TKT down-  
396 regulation could be a late and adaptive process, aimed at limiting a further development of fat  
397 mass. Immunostaining methods showed for the first time the expression of TKT in human  
398 omental adipose tissue. TKT, an ubiquitous enzyme engaged in multiple metabolic pathways,  
399 was widely distributed in adipocytes as well as other stromal cells. TKT was present mainly in  
400 the cytoplasm of adipose cells, but a few nuclei also expressed the protein. Interestingly, the  
401 nuclei of human pre-adipocytes expressed TKT in contrast to fully differentiated adipocytes, in  
402 which TKT was only observed in the cytoplasm. A nuclear localization of TKT had already  
403 been described [33]; in this regard, it is interesting to mention that in a highly proliferative state

404 increased cell division rate would require large amounts of phosphate pentose, which would  
405 account for the nuclear localization of TKT. On the other hand, mature adipocytes keep pentose  
406 phosphate consumption to a minimum while consuming many NADPH molecules for  
407 lipogenesis, which would explain TKT localization in the cytoplasm of mature adipocytes.  
408 Taken together, these findings highlight the potential role of this protein in adipose tissue and  
409 adipogenesis.

410 2D-DIGE and immunoblotting analyses have shown significant down-regulation of  
411 aminoacylase-1 (ACY-1) with obesity. ACY-1 is a cytosolic, homodimeric, zinc-binding  
412 enzyme that function in the catabolism and retrieval of acylated amino acids. ACY-1 expression  
413 has been found associated to renal carcinoma [34] and to an inborn metabolic disorder [35].  
414 Nevertheless, this is the first report on ACY-1 expression in human fat. The nuclear localization  
415 of ACY-1 is striking. In agreement with our finding, this enzyme had been previously found in  
416 the nucleus of rat normal proximal tubular cells [34]. It is possible that several unidentified  
417 nuclear proteins are substrates for ACY-1. It is noteworthy that ACY-1 physically interacts and  
418 functionally modulates sphingosine kinase 1, SPHK1 [36], a lipid kinase that converts  
419 sphingosine and ATP to sphingosine-1-phosphate (S1P). S1P is a potent signalling molecule  
420 involved in angiogenesis and cell growth among other cellular processes [37]. Of note, we have  
421 shown that both ACY-1 and SPHK1 are associated with adipogenesis in 3T3-L1 cells (Fig. 6  
422 and Supplemental Fig. 4) as already found with the latter [38]. These results collectively support  
423 the hypothesis that the SPHK1/ACY-1 system could play a role in obesity. Further studies are  
424 underway to explore ACY-1 functional role in adipose tissue.

425 Our results based on the 3T3-L1 adipocytes differentiation process have shown for the first time  
426 an increment of ACY-1 and TKT levels. Long-lasting fat excess has been evidenced to reduce  
427 adipogenesis in adipose tissue to limit further expansion of fat mass [8-11]. We hypothesize that  
428 the diminished levels of ACY-1 and TKT proteins in obesity stem from the impaired adipogenic  
429 capacity of obese adipocytes.

430 The proteomic analysis has enabled the identification of other relevant proteins involved in  
431 obesity or whose expression in fat has been widely documented. Results revealed the over-



432 expression in obese subjects of HSP70. HSPs not only serve as chaperones, mainly controlling  
433 protein folding of newly translated polypeptides but also protect cells against many chronically  
434 and acutely stressful conditions [39]. In spite of the numerous cellular processes in which  
435 HSP70 takes part, it can be hypothesized that the higher levels of HSP70 found in the omental  
436 fat from obese patients would serve to reduce the cellular stress associated to obesity. In skeletal  
437 muscle, evidences have shown that there is a decreased expression of HSP70 in type 2 diabetes  
438 patients [40, 41] and in mice models an elevation of HSP70 protected against obesity-induced  
439 hyperglycemia, hyperinsulinemia, glucose intolerance and insulin resistance [41]. Nevertheless,  
440 no similar studies have been conducted in adipose tissue to date. We performed Western Blot  
441 analyses to compare omental fat samples from obese patients with and without type 2 diabetes.  
442 Interestingly, in agreement with these evidences, our results revealed that the amount of HSP70  
443 was significantly lower in type 2 diabetes obese subjects than in obese without type 2 diabetes  
444 ( $p=0.007$ ), as illustrated in Supplemental Fig. 5. Therefore this result supports a protection role  
445 for HSP70.

446 It is well established that monoamine oxidase A (MAOA), a mitochondrial enzyme involved in  
447 the oxidative deamination catabolism of neurotransmitters and exogenous amines, is highly  
448 expressed in the adipocyte-enriched fraction of human adipose tissue [42]. Our results showed  
449 reduced levels of MAOA in obese subjects, which is in agreement with an earlier report  
450 revealing reduced MAOA activity in the adipose tissue from obese subjects [43]. Our study also  
451 showed reduced expression levels of FABP5 in obese individuals, in consistence with previous  
452 studies in subcutaneous fat [44]. FABP5 is a relevant adipose tissue protein that facilitates lipid  
453 usage in metabolic pathways and plays a role in metabolic syndrome, insulin resistance, type 2  
454 diabetes, and atherosclerosis, as elucidated in studies based on genetically modified mice [45].  
455 Mice lacking FABP5 was protected against diet-induced obesity, insulin resistance and other  
456 related diseases [46]. Ongoing studies in our laboratory attempt to evaluate whether these  
457 results might be extrapolated to humans.

458

459 In summary, this work is, to our knowledge, the first proteomic study on omental fat comparing  
460 non-obese and obese people and represents one of the few proteomic analyses in human adipose  
461 tissue. Our findings evidence a clearly distinctive biological profile of obese and non-obese  
462 subjects highlighting a noticeably decreased expression of proteins related to metabolic  
463 processes and an increased expression of proteins that develop structural functions in the cell in  
464 response to obesity. Besides, our study has revealed that TKT and ACY-1 are promising new  
465 players involved in obesity. Our results will strengthen the understanding of molecular  
466 pathogenesis of obesity, whilst the identified proteins can be regarded as potential targets for  
467 future therapeutic strategies.

468

469

#### 470 **Acknowledgements**

471 This work was supported by Grants SAF-2009-10461 (to B.P.), SAF-2008-02073 (to J.M.F.R.)  
472 from the Ministerio de Ciencia e Innovación de España and from the Fundación Mutua  
473 Madrileña (to B.P.). The CNIC is supported by the Ministerio de Ciencia e Innovación and the  
474 Pro CNIC Foundation. CIBER is an initiative from the Instituto de Salud Carlos III. We  
475 acknowledge the technical assistance of Ana de la Encarnación, Pablo Parra and Alba  
476 Moratalla.

477

#### 478 **Appendix A. Supplementary data**

479 Supplementary data associated with this article contains Supplemental Fig. 1, 2, 3, 4 and 5,  
480 Supplemental Table 1 and Supplemental Table 2, and can be found in the online version.

481

482

- 484 [1] Daniels SR, Jacobson MS, McCrindle BW, Eckel RH, Sanner BM. American Heart  
485 Association Childhood Obesity Research Summit Report. *Circulation*. 2009;119:e489-  
486 517.
- 487 [2] Calle EE, Kaaks R. Overweight, obesity and cancer: epidemiological evidence and  
488 proposed mechanisms. *Nat Rev Cancer*. 2004;4:579-91.
- 489 [3] Spiegelman BM, Flier JS. Obesity and the regulation of energy balance. *Cell*.  
490 2001;104:531-43.
- 491 [4] Montague CT, O'Rahilly S. The perils of portliness: causes and consequences of  
492 visceral adiposity. *Diabetes*. 2000;49:883-8.
- 493 [5] Rebuffe-Scrive M, Andersson B, Olbe L, Bjorntorp P. Metabolism of adipose tissue  
494 in intraabdominal depots of nonobese men and women. *Metabolism*. 1989;38:453-8.
- 495 [6] Matsuzawa Y. Therapy Insight: adipocytokines in metabolic syndrome and related  
496 cardiovascular disease. *Nat Clin Pract Cardiovasc Med*. 2006;3:35-42.
- 497 [7] Keller MP, Attie AD. Physiological insights gained from gene expression analysis in  
498 obesity and diabetes. *Annu Rev Nutr*. 2010;30:341-64.
- 499 [8] Nadler ST, Stoehr JP, Schueler KL, Tanimoto G, Yandell BS, Attie AD. The  
500 expression of adipogenic genes is decreased in obesity and diabetes mellitus. *Proc Natl*  
501 *Acad Sci U S A*. 2000;97:11371-6.
- 502 [9] Gomez-Ambrosi J, Catalan V, Diez-Caballero A, Martinez-Cruz LA, Gil MJ,  
503 Garcia-Foncillas J, et al. Gene expression profile of omental adipose tissue in human  
504 obesity. *FASEB J*. 2004;18:215-7.
- 505 [10] Ortega FJ, Mayas D, Moreno-Navarrete JM, Catalan V, Gomez-Ambrosi J, Esteve  
506 E, et al. The gene expression of the main lipogenic enzymes is downregulated in  
507 visceral adipose tissue of obese subjects. *Obesity (Silver Spring)*. 2010;18:13-20.
- 508 [11] Dubois SG, Heilbronn LK, Smith SR, Albu JB, Kelley DE, Ravussin E. Decreased  
509 expression of adipogenic genes in obese subjects with type 2 diabetes. *Obesity (Silver*  
510 *Spring)*. 2006;14:1543-52.
- 511 [12] Wang MY, Grayburn P, Chen S, Ravazzola M, Orci L, Unger RH. Adipogenic  
512 capacity and the susceptibility to type 2 diabetes and metabolic syndrome. *Proc Natl*  
513 *Acad Sci U S A*. 2008;105:6139-44.
- 514 [13] Peral B, Camafeita E, Fernandez-Real JM, Lopez JA. Tackling the human adipose  
515 tissue proteome to gain insight into obesity and related pathologies. *Expert Rev*  
516 *Proteomics*. 2009;6:353-61.
- 517 [14] Perez-Perez R, Ortega-Delgado FJ, Garcia-Santos E, Lopez JA, Camafeita E,  
518 Ricart W, et al. Differential proteomics of omental and subcutaneous adipose tissue  
519 reflects their unlike biochemical and metabolic properties. *J Proteome Res*.  
520 2009;8:1682-93.
- 521 [15] Peinado JR, Jimenez-Gomez Y, Pulido MR, Ortega-Bellido M, Diaz-Lopez C,  
522 Padillo FJ, et al. The stromal-vascular fraction of adipose tissue contributes to major  
523 differences between subcutaneous and visceral fat depots. *Proteomics*. 2010;10:3356-  
524 66.
- 525 [16] Kheterpal I, Ku G, Coleman L, Yu G, Ptitsyn AA, Floyd ZE, et al. Proteome of  
526 Human Subcutaneous Adipose Tissue Stromal Vascular Fraction Cells versus Mature  
527 Adipocytes Based on DIGE. *J Proteome Res*. 2011;10:1519-27.
- 528 [17] Corton M, Botella-Carretero JI, Lopez JA, Camafeita E, San Millan JL, Escobar-  
529 Morreale HF, et al. Proteomic analysis of human omental adipose tissue in the

530 polycystic ovary syndrome using two-dimensional difference gel electrophoresis and  
531 mass spectrometry. *Hum Reprod.* 2008;23:651-61.

532 [18] Shevchenko A, Tomas H, Havlis J, Olsen JV, Mann M. In-gel digestion for mass  
533 spectrometric characterization of proteins and proteomes. *Nat Protoc.* 2006;1:2856-60.

534 [19] Suckau D, Resemann A, Schuerenberg M, Hufnagel P, Franzen J, Holle A. A novel  
535 MALDI LIFT-TOF/TOF mass spectrometer for proteomics. *Anal Bioanal Chem.*  
536 2003;376:952-65.

537 [20] Perkins DN, Pappin DJ, Creasy DM, Cottrell JS. Probability-based protein  
538 identification by searching sequence databases using mass spectrometry data.  
539 *Electrophoresis.* 1999;20:3551-67.

540 [21] Ortega FJ, Vazquez-Martin A, Moreno-Navarrete JM, Bassols J, Rodriguez-  
541 Hermosa J, Girones J, et al. Thyroid hormone responsive Spot 14 increases during  
542 differentiation of human adipocytes and its expression is down-regulated in obese  
543 subjects. *Int J Obes (Lond).* 2010;34:487-99.

544 [22] Despres JP, Lemieux I. Abdominal obesity and metabolic syndrome. *Nature.*  
545 2006;444:881-7.

546 [23] Henegar C, Tordjman J, Achard V, Lacasa D, Cremer I, Guerre-Millo M, et al.  
547 Adipose tissue transcriptomic signature highlights the pathological relevance of  
548 extracellular matrix in human obesity. *Genome Biol.* 2008;9:R14.

549 [24] Marrades MP, Gonzalez-Muniesa P, Arteta D, Martinez JA, Moreno-Aliaga MJ.  
550 Orchestrated downregulation of genes involved in oxidative metabolic pathways in  
551 obese vs. lean high-fat young male consumers. *J Physiol Biochem.* 2011;67:15-26.

552 [25] Wilson-Fritch L, Burkart A, Bell G, Mendelson K, Leszyk J, Nicoloso S, et al.  
553 Mitochondrial biogenesis and remodeling during adipogenesis and in response to the  
554 insulin sensitizer rosiglitazone. *Mol Cell Biol.* 2003;23:1085-94.

555 [26] Rong JX, Qiu Y, Hansen MK, Zhu L, Zhang V, Xie M, et al. Adipose  
556 mitochondrial biogenesis is suppressed in db/db and high-fat diet-fed mice and  
557 improved by rosiglitazone. *Diabetes.* 2007;56:1751-60.

558 [27] Patti ME, Corvera S. The role of mitochondria in the pathogenesis of type 2  
559 diabetes. *Endocr Rev.* 2010;31:364-95.

560 [28] Koh EH, Park JY, Park HS, Jeon MJ, Ryu JW, Kim M, et al. Essential role of  
561 mitochondrial function in adiponectin synthesis in adipocytes. *Diabetes.* 2007;56:2973-  
562 81.

563 [29] Shi X, Burkart A, Nicoloso SM, Czech MP, Straubhaar J, Corvera S. Paradoxical  
564 effect of mitochondrial respiratory chain impairment on insulin signaling and glucose  
565 transport in adipose cells. *J Biol Chem.* 2008;283:30658-67.

566 [30] Poussin C, Hall D, Minehira K, Galzin AM, Tarussio D, Thorens B. Different  
567 transcriptional control of metabolism and extracellular matrix in visceral and  
568 subcutaneous fat of obese and rimonabant treated mice. *PLoS One.* 2008;3:e3385.

569 [31] Schenk G, Duggleby RG, Nixon PF. Properties and functions of the thiamin  
570 diphosphate dependent enzyme transketolase. *Int J Biochem Cell Biol.* 1998;30:1297-  
571 318.

572 [32] Xu ZP, Wawrousek EF, Piatigorsky J. Transketolase haploinsufficiency reduces  
573 adipose tissue and female fertility in mice. *Mol Cell Biol.* 2002;22:6142-7.

574 [33] Joshi S, Singh AR, Kumar A, Misra PC, Siddiqi MI, Saxena JK. Molecular cloning  
575 and characterization of *Plasmodium falciparum* transketolase. *Mol Biochem Parasitol.*  
576 2008;160:32-41.

577 [34] Zhong Y, Onuki J, Yamasaki T, Ogawa O, Akatsuka S, Toyokuni S. Genome-wide  
578 analysis identifies a tumor suppressor role for aminoacylase 1 in iron-induced rat renal  
579 cell carcinoma. *Carcinogenesis.* 2009;30:158-64.

580 [35] Sass JO, Mohr V, Olbrich H, Engelke U, Horvath J, Fliegau M, et al. Mutations in  
581 ACY1, the gene encoding aminoacylase 1, cause a novel inborn error of metabolism.  
582 *Am J Hum Genet.* 2006;78:401-9.

583 [36] Maceyka M, Nava VE, Milstien S, Spiegel S. Aminoacylase 1 is a sphingosine  
584 kinase 1-interacting protein. *FEBS Lett.* 2004;568:30-4.

585 [37] Allende ML, Yamashita T, Proia RL. G-protein-coupled receptor S1P1 acts within  
586 endothelial cells to regulate vascular maturation. *Blood.* 2003;102:3665-7.

587 [38] Hashimoto T, Igarashi J, Kosaka H. Sphingosine kinase is induced in mouse 3T3-  
588 L1 cells and promotes adipogenesis. *J Lipid Res.* 2009;50:602-10.

589 [39] Calderwood SK, Khaleque MA, Sawyer DB, Ciocca DR. Heat shock proteins in  
590 cancer: chaperones of tumorigenesis. *Trends Biochem Sci.* 2006;31:164-72.

591 [40] Kurucz I, Morva A, Vaag A, Eriksson KF, Huang X, Groop L, et al. Decreased  
592 expression of heat shock protein 72 in skeletal muscle of patients with type 2 diabetes  
593 correlates with insulin resistance. *Diabetes.* 2002;51:1102-9.

594 [41] Chung J, Nguyen AK, Henstridge DC, Holmes AG, Chan MH, Mesa JL, et al.  
595 HSP72 protects against obesity-induced insulin resistance. *Proc Natl Acad Sci U S A.*  
596 2008;105:1739-44.

597 [42] Pizzinat N, Marti L, Remaury A, Leger F, Langin D, Lafontan M, et al. High  
598 expression of monoamine oxidases in human white adipose tissue: evidence for their  
599 involvement in noradrenaline clearance. *Biochem Pharmacol.* 1999;58:1735-42.

600 [43] Visentin V, Prevot D, De Saint Front VD, Morin-Cussac N, Thalamas C, Galitzky  
601 J, et al. Alteration of amine oxidase activity in the adipose tissue of obese subjects.  
602 *Obes Res.* 2004;12:547-55.

603 [44] Fisher RM, Hoffstedt J, Hotamisligil GS, Thorne A, Ryden M. Effects of obesity  
604 and weight loss on the expression of proteins involved in fatty acid metabolism in  
605 human adipose tissue. *Int J Obes Relat Metab Disord.* 2002;26:1379-85.

606 [45] Furuhashi M, Hotamisligil GS. Fatty acid-binding proteins: role in metabolic  
607 diseases and potential as drug targets. *Nat Rev Drug Discov.* 2008;7:489-503.

608 [46] Maeda K, Cao H, Kono K, Gorgun CZ, Furuhashi M, Uysal KT, et al.  
609 Adipocyte/macrophage fatty acid binding proteins control integrated metabolic  
610 responses in obesity and diabetes. *Cell Metab.* 2005;1:107-19.

611

612

613

614 **Figure Legends**

615

616 **Fig. 1.** Representative silver stained 2D gel of omental adipose tissue proteins using 24 cm pH3-  
617 11NL (left to right) strips in the first dimension and 12% PAGE-SDS gels in the second  
618 dimension. Numbers correspond to differentially expressed protein spots as indicated in Table  
619 1. Supplemental Fig. 1 provides a more convenient visualization of the differential protein spots  
620 on the silver stained 2D gel.

621

622 **Fig. 2.** Pie chart representations of PANTHER Biological Process and Molecular Function  
623 classes significantly over-represented in the set of downregulated proteins (A, C) and in the set  
624 of up-regulated proteins (B, D) in obesity. Classes with no significant P-value are displayed in  
625 grey colour for comparative purposes (note that the class *Generation of Precursor Metabolites*  
626 *and Energy* has no representation in the group of proteins increased in obesity). It should be  
627 pointed that PANTHER may attribute multiple classes to a given protein.

628

629 **Fig. 3.** TKT, ACY-1 and HSP70 expression in human omental adipose tissue. Standardized  
630 abundance was determined by DeCyder analysis of 2D-DIGE data from non-obese and obese  
631 fat samples. The (+) and (-) symbols indicate increased and decreased levels with respect to the  
632 internal standard, respectively (A). Representative **Western Blot** analysis of TKT, ACY-1 and  
633 HSP70 expression from non-obese and obese fat samples. The results were normalized for B-  
634 actin density (B). Values for relative intensity obtained after densitometry of the bands are  
635 means +/- SD (C). Representative images of four independent analyses.

636

637 **Fig. 4.** Immunofluorescence staining of TKT in human omental adipose tissue, human pre-  
638 adipocytes and human adipocytes differentiated *in vitro*. In fat biopsies TKT is mainly shown in  
639 the cytosol of adipocytes and other SVF cells, but is also observed in the nuclei of a few cells  
640 (four white circles) (A). In human pre-adipocytes TKT is shown both in the cytoplasm and the  
641 nucleus (B). In human differentiated adipocytes TKT is exclusively observed in the cytosol (C).

642 Images are representative of adipose tissue sections collected from three subjects (A) and three  
643 replicates (B and C).

644

645 **Fig. 5.** Immunofluorescence staining of ACY-1 in human omental pre-adipocytes and  
646 adipocytes differentiated *in vitro*. ACY-1 (in red) is shown in the nucleus of pre-adipocytes (day  
647 0) (A). In differentiated adipocytes (day 14) ACY-1 is observed in the cytosol and to a lesser  
648 extent in the nucleus (B). Close-up view of a differentiated adipocyte showing ACY-1 around  
649 the lipid droplets (C). The counterstaining of nuclei (DAPI) is shown in blue. Lipid droplets  
650 have been stained with BODIPY 493/503 (in green). Images are representative of three  
651 replicates.

652

653 **Fig. 6.** TKT and ACY-1 and protein levels assessed by Western Blot during adipogenic  
654 maturation of 3T3-L1 (A). Values for relative intensity obtained after densitometry of the bands  
655 are means  $\pm$  SD. \*  $p < 0.005$  and \*\*  $p < 0.05$  for comparisons between TKT, and ACY-1 levels  
656 at day 9 vs. day 0, respectively (B). FABP4 was used as an adipogenesis control. The results  
657 were normalized for GAPDH density. Representative images of three independent analyses.

658

659 **Table 1.** Proteins identified by MALDI-MS showing significantly regulated expression in the  
660 omental fat from morbidly obese ( $n=6$ ) and non-obese ( $n=6$ ) individuals. Protein identification  
661 details are illustrated in Supplemental Table 1.





Table 1. Proteins identified by MALDI-MS showing significantly regulated expression in the omental fat from obese and non-obese individuals

DIGE			Protein			Mascot						
Spot <sup>a</sup>	p-value <sup>b</sup>	Av. Ratio <sup>c</sup>	Accession <sup>d</sup>	Locus <sup>e</sup>	Name	Score <sup>f</sup>	Expect <sup>g</sup>	ions score <sup>h</sup>	kDa theor <sup>i</sup>	pI theor <sup>j</sup>	Match pept <sup>k</sup>	Cover % <sup>l</sup>
1	1.6E-02	1.6	gi 642534	AAA85268	lumican	191	7.90E-13	102	38.7	6.2	5	14
2	8.0E-03	-2.0	gi 62414289	NP_003371	vimentin	273	4.90E-21		53.7	5.1	19	47
3	1.2E-02	2.2	gi 24234699	NP_002267	keratin 19	372	6.30E-31	157	44.1	5.0	18	43
4	1.4E-02	2.2	gi 42734430	NP_036364	polymerase I and transcript release factor	164	3.90E-10	73	43.5	5.5	6	12
5	3.9E-03	2.2	gi 24234699	NP_002267	keratin 19	257	2.00E-19		44.1	5.0	16	39
6	3.0E-02	1.7	gi 42734430	NP_036364	polymerase I and transcript release factor	129	2.80E-08	82	43.5	5.5	6	11
			gi 18645167	AAH23990	annexin A2	136	5.60E-09		38.8	7.6	9	28
7	2.1E-02	1.5	gi 167614506	NP_002289	L-plastin	235	3.10E-17	137	70.8	5.3	11	22
			gi 2897116	AAC39708	integrin alpha-7	157	2.00E-09	85	125.4	5.6	9	10
			gi 50415798	AAH78178	lamin-B1	129	1.20E-06		38.3	5.4	9	30
8	3.6E-02	2.1	gi 55962552	CAI18465	heat shock 70kDa protein 1A	181	7.80E-12	85	52.2	5.4	7	13
9	3.3E-02	1.7	gi 3127926	CAA36267	collagen type VI, alpha 3 chain	89	1.30E-02	91	345.1	6.4	8	3
10	4.2E-02	1.6	gi 42734430	NP_036364	polymerase I and transcript release factor	157	2.00E-09	74	43.5	5.5	6	12
11	5.5E-03	1.8	gi 62898171	BAD97025	L-plastin variant	240	9.90E-18	103	70.8	5.2	10	18
12	2.0E-02	1.6	gi 119626083	EAX05678	albumin, isoform CRA_t	168	1.60E-10		60.2	6.7	14	27
13	1.2E-02	2.1	gi 4506925	NP_003013	SH3 domain binding glutamic acid-rich protein like	87	4.60E-04	69	12.8	5.2	1	8
14	4.7E-02	1.4	gi 42476013	NP_940916	NHL repeat containing 2	114	3.90E-05	57	80.2	5.3	4	6
15	6.3E-03	2.6	gi 25777732	NP_000681	mitochondrial aldehyde dehydrogenase 2 precursor	312	6.30E-25	149	56.9	6.6	11	22
16	4.3E-02	-1.5	gi 91992949	AAI14619	guanine nucleotide-binding protein beta subunit	161	7.80E-10	77	37.1	5.6	5	16
17	3.0E-02	1.6	gi 181573	AAA35763	cytokeratin 8	147	2.00E-08	82	53.5	5.5	5	10
18	5.8E-05	2.7	gi 67782365	NP_005547	keratin 7	293	4.90E-23	133	51.4	5.4	15	30
19	2.2E-02	1.5	gi 4096652	AAC99987	aryl sulfotransferase	102	1.40E-05	82	34.3	5.8	1	3
20	2.7E-03	2.0	gi 2781209	1FZA_C	fibrinogen gamma chain	240	9.90E-18	128	36.5	5.9	7	33
21	3.1E-02	1.9	gi 4502101	NP_000691	annexin I	187	2.00E-12	105	38.9	6.6	5	17
22	3.1E-03	2.3	gi 1419564	CAA67203	keratin 8, isoform CRA_d	115	3.10E-05	81	30.8	5.0	2	8
23	1.9E-03	-2.1	gi 662841	AAA62175	heat shock protein 27	126	2.50E-06	93	22.4	7.8	2	13
24	4.8E-03	1.6	gi 168988718	2VDB_A	serum albumin	161	7.80E-10		67.8	5.6	12	18
25	1.1E-03	2.6	gi 237823916	3GHG_C	chain C, human fibrinogen	396	2.50E-33	216	47.0	5.5	14	51
			gi 181573	AAA35763	cytokeratin 8	366	2.50E-30	186	53.5	5.5	15	37
26	2.0E-03	-1.5	gi 4501901	NP_000657	aminoacylase 1	190	9.90E-13	60	46.1	5.8	8	18
27	1.6E-03	1.5	gi 18645167	AAH23990	annexin A2	185	3.10E-12	69	38.8	7.6	7	20
28	1.2E-02	-1.7	gi 4557581	NP_001435	fatty acid binding protein 5 (psoriasis-associated)	277	2.00E-21	88	15.5	6.6	10	68
29	3.1E-02	1.8	gi 119626066	EAX05661	albumin, isoform CRA_c	141	7.80E-08		27.7	6.4	8	30
30	4.4E-02	1.9	gi 17389815	AAH17917	triosephosphate isomerase 1	131	7.80E-07		26.9	6.5	7	32
31	1.1E-02	-1.7	gi 4557233	NP_000008	short-chain acyl-CoA dehydrogenase precursor	119	1.20E-05		44.6	8.1	7	19
32	3.9E-02	-1.5	gi 157168362	NP_000261	nucleoside phosphorylase	123	4.90E-06	71	32.3	6.5	3	14
33	3.1E-02	-1.8	gi 110590599	2HAV_A	serotransferrin precursor	119	1.20E-05		77.0	6.9	9	17
34	6.3E-03	-1.5	gi 4557231	NP_000007	medium-chain acyl-CoA dehydrogenase isoform a precursor	158	1.60E-09	91	47.0	8.6	4	13
35	2.1E-03	-1.5	gi 119631279	EAX10874	3-hydroxyisobutyryl-coenzyme A hydrolase, isoform CRA_b	159	1.20E-09		49.4	9.4	9	23
36	3.2E-02	-1.5	gi 4502517	NP_001729	carbonic anhydrase I	141	1.80E-09	72	28.9	6.6	4	21
37	3.1E-02	1.4	gi 27436946	NP_733821	lamin A/C isoform 1 precursor	521	7.80E-46	232	74.4	6.6	22	38

38	4.8E-03	-1.5	gij119590499	EAW70093	fumarate hidratase, isoform CRA_d	174	3.90E-11	136	46.6	6.9	2	6
39	6.0E-05	-1.7	gij189181759	NP_001121188	electron transfer flavoprotein, alpha polypeptide isoform b	167	4.50E-12	93	30.2	8.8	4	20
40	4.3E-02	-1.4	gij4557735	NP_000231	monoamine oxidase A	126	2.50E-06	69	60.2	7.9	4	11
41	1.0E-02	-1.9	gij30583667	AAP36082	citrate synthase	109	1.20E-04	69	29.6	7.8	2	7
42	1.1E-02	-1.6	gij71296885	AAH44787	monoamine oxidase A	146	2.50E-08	66	60.2	6.9	6	15
43	4.3E-03	-1.4	gij4557014	NP_001743	catalase	278	1.60E-21	115	59.9	6.9	9	25
44	1.3E-02	-1.5	gij388891	AAA61222	transketolase	150	9.90E-09		68.5	7.9	10	22
45	3.2E-03	-1.6	gij179950	AAB59522	catalase	195	3.10E-13	70	51.6	7.8	8	23
46	3.1E-03	-1.8	gij223002	0401173A	fibrin beta	170	9.90E-11		51.4	8.0	10	26
47	1.4E-04	-1.6	gij48257138	AAH00105	citrate synthase, mitochondrial precursor	211	7.80E-15	101	45.8	6.5	6	16
48	3.0E-02	-1.7	gij388891	AAA61222	transketolase	178	1.60E-11		68.5	7.9	10	25
49	1.0E-02	-1.5	gij4557237	NP_000010	acetyl-coenzyme A acetyltransferase 1 precursor	129	1.20E-06	95	45.5	9.0	2	7
50	8.8E-03	-1.5	gij13111901	AAH03119	ATP synthase subunit alpha, mitochondrial precursor	101	1.80E-05	86	40.4	8.9	1	3
51	1.8E-02	-1.4	gij16950633	NP_446464	argininosuccinate synthetase 1	180	9.90E-12	49	46.8	8.1	7	16
52	1.7E-02	-1.7	gij598143	AAB48003	alcohol dehydrogenase beta-3 subunit	220	9.90E-16		40.7	8.5	12	32
53	2.7E-02	2.0	gij4757756	NP_004030	annexin A2 isoform 2	283	4.90E-22	87	38.8	7.6	15	48
54	1.9E-02	-1.6	gij119626625	EAX06220	L-3-hydroxyacyl-coenzyme A dehydrogenase short chain isoform CRA_c	170	9.90E-11	78	7.6	9.3	4	52
55	4.1E-02	-1.6	gij598143	AAB48003	alcohol dehydrogenase beta-3 subunit	212	6.20E-15	63	40.7	8.5	10	28
56	3.5E-02	-1.5	gij40807491	NP_001986	acyl-CoA synthetase long-chain family member 1	306	2.50E-24	141	78.9	6.8	11	20

<sup>a</sup>Spot numbering as shown in 2-DE silver gel in Figure 1. <sup>b</sup>*p*-value of the Student t-test and <sup>c</sup>average volumen ratio (Obese/non-Obese) as calculated by the DeCyder analysis. <sup>d</sup>Protein and <sup>e</sup>locus accesion codes from the NCBI database. <sup>f</sup>Mascot score, <sup>g</sup>Mascot expected value, <sup>h</sup>Mascot Ions score, <sup>i</sup>theoretical molecular weight (kDa) and <sup>j</sup>*pI*, <sup>k</sup>number of matched peptides and <sup>l</sup>protein sequence coverage for the most probable candidate as provided by Mascot. Protein identification details (MS and MS/MS spectra) are listed in Supplemental Table 1.

Fig.1 Silver stained 2D-gel  
[Click here to download high resolution image](#)

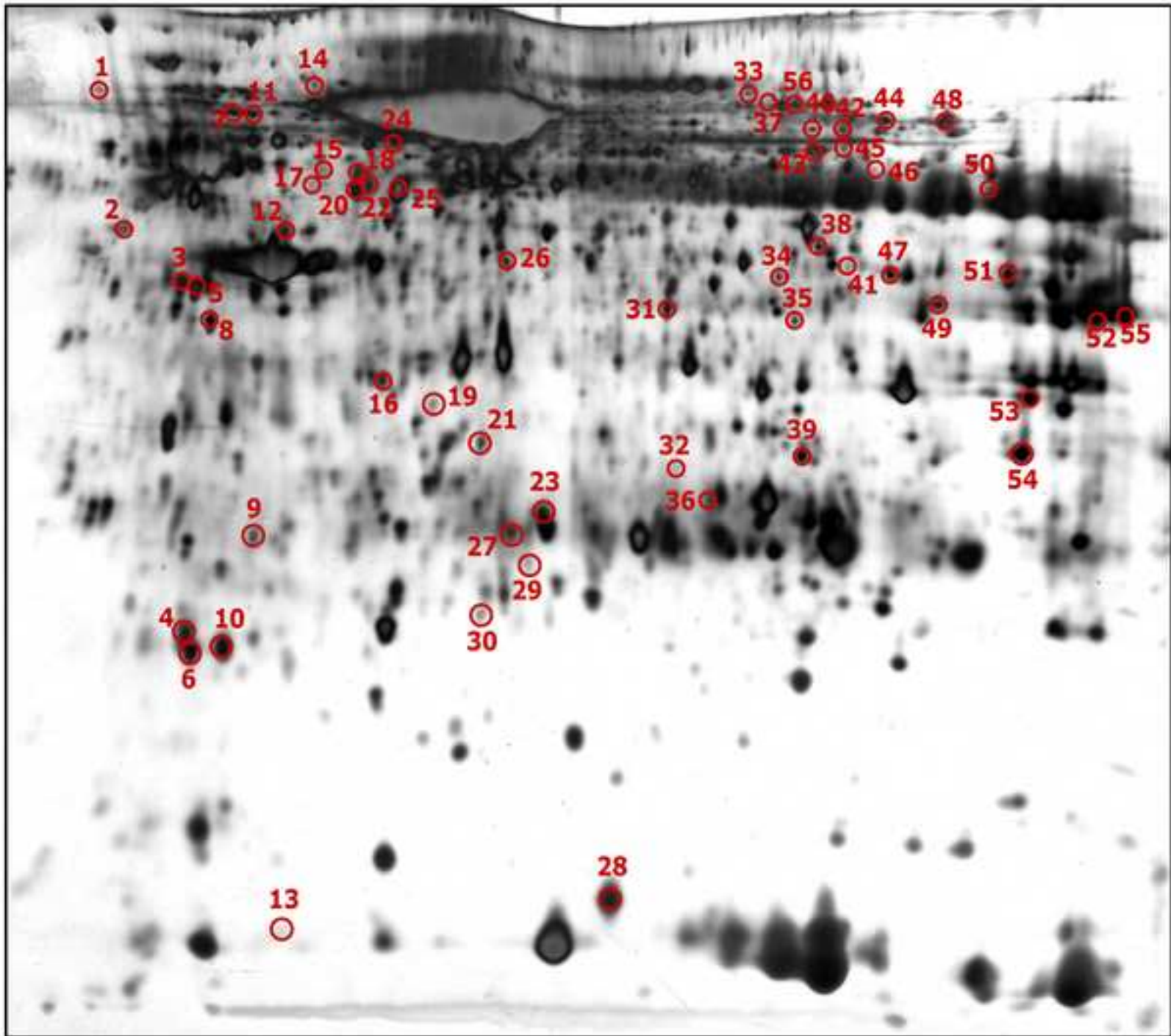
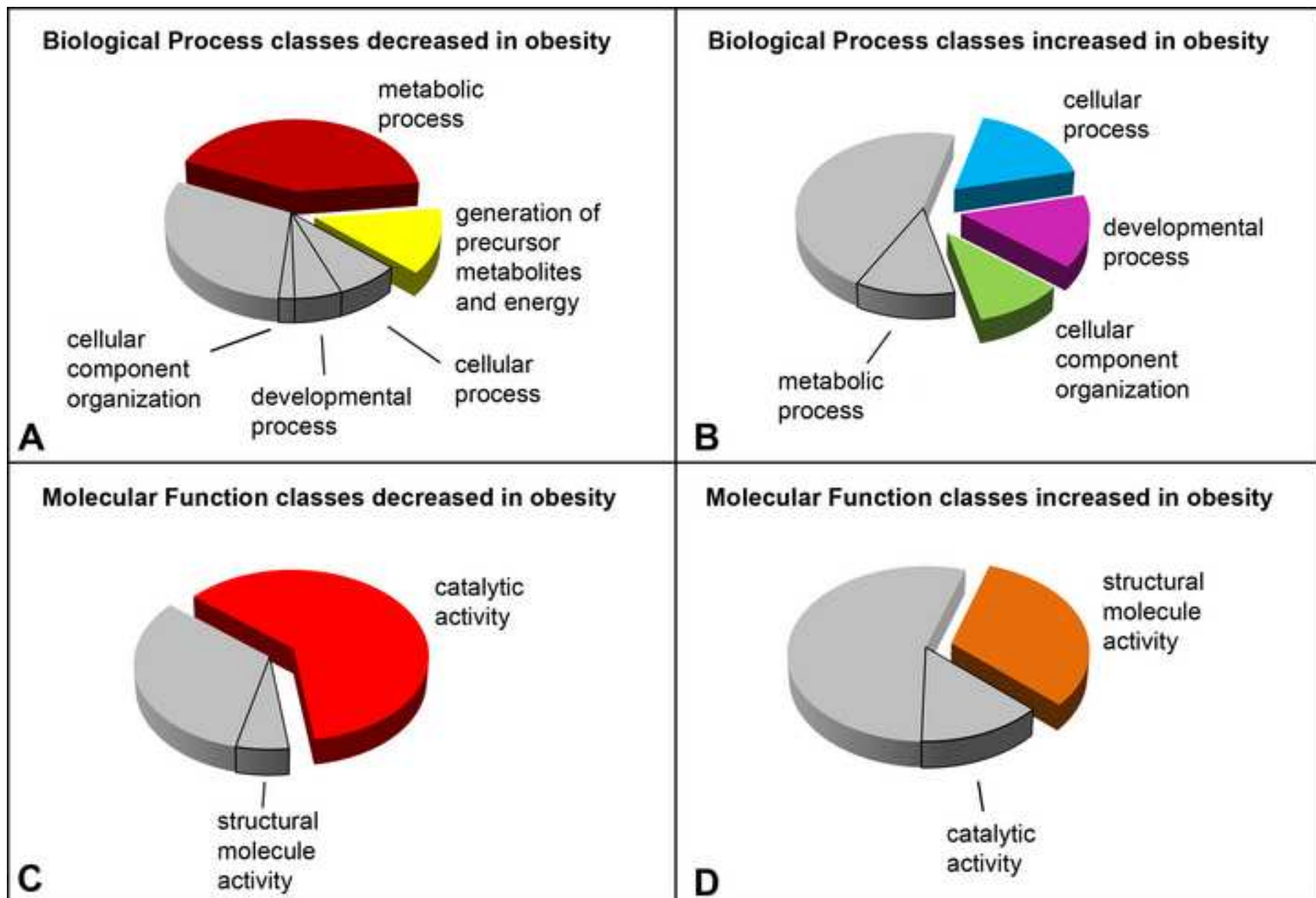


Fig2. Pie chart representations of PANTHER  
[Click here to download high resolution image](#)



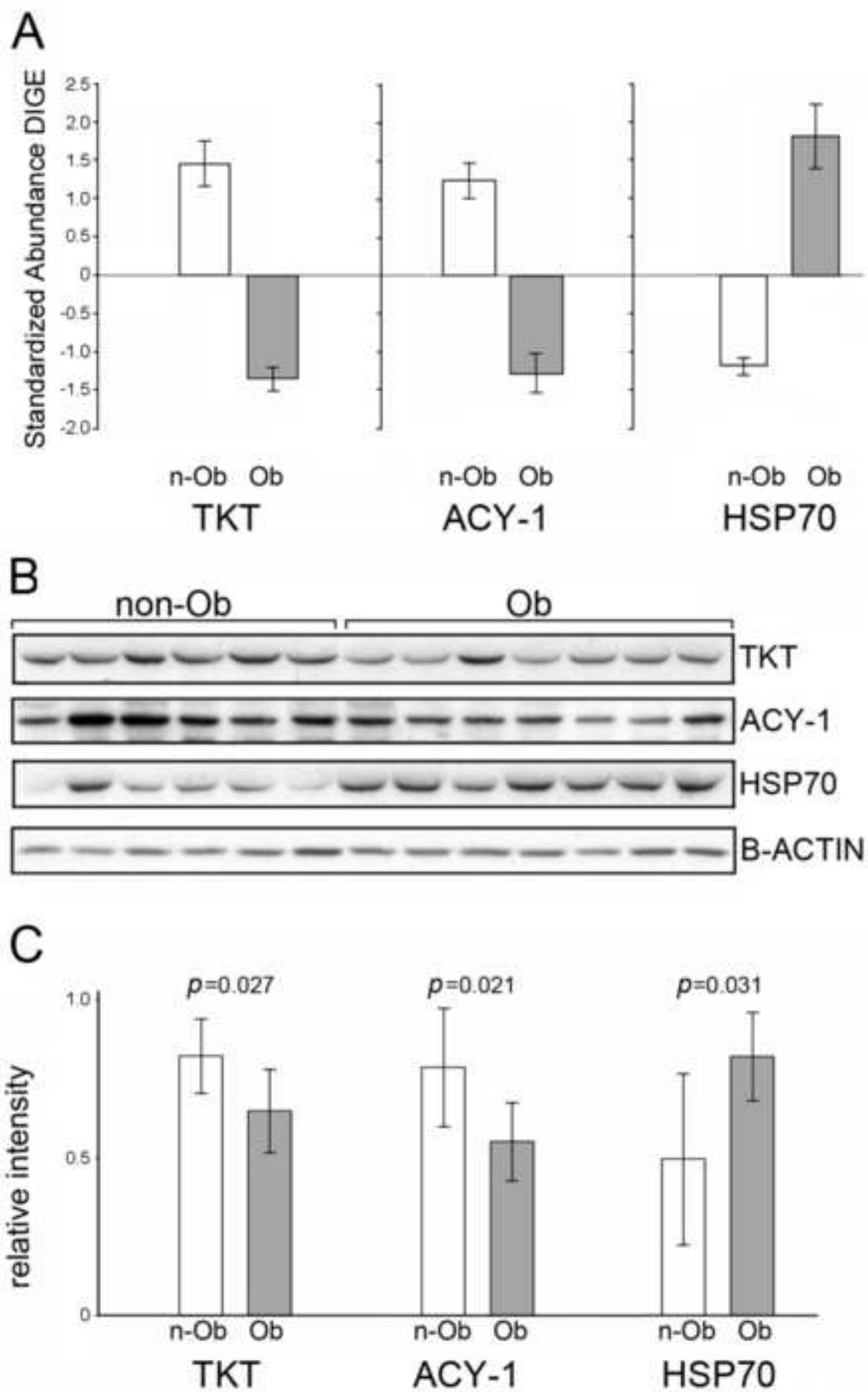
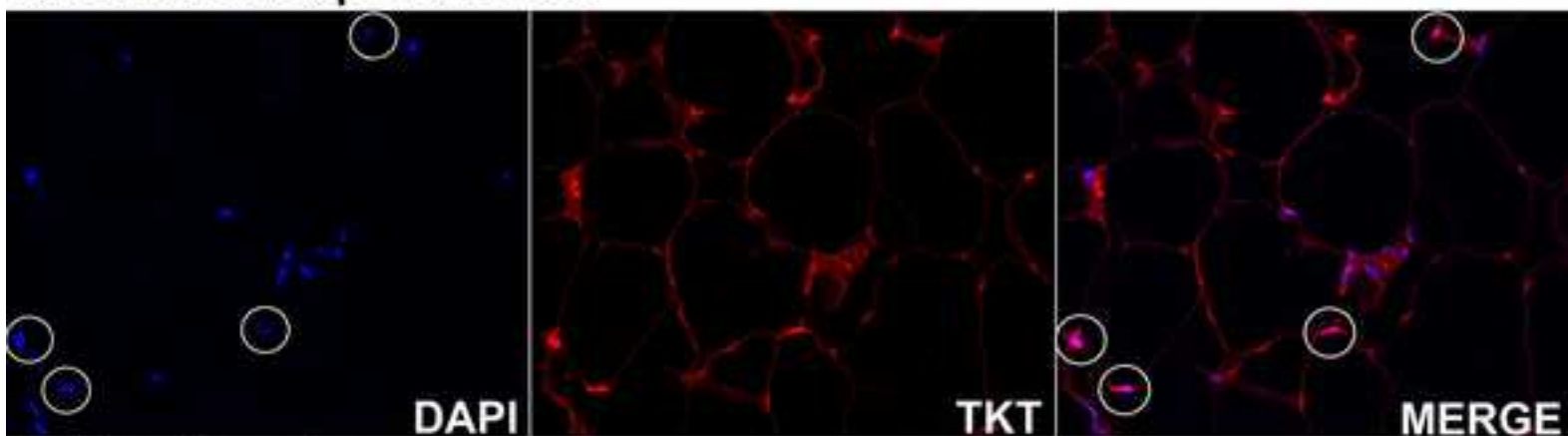
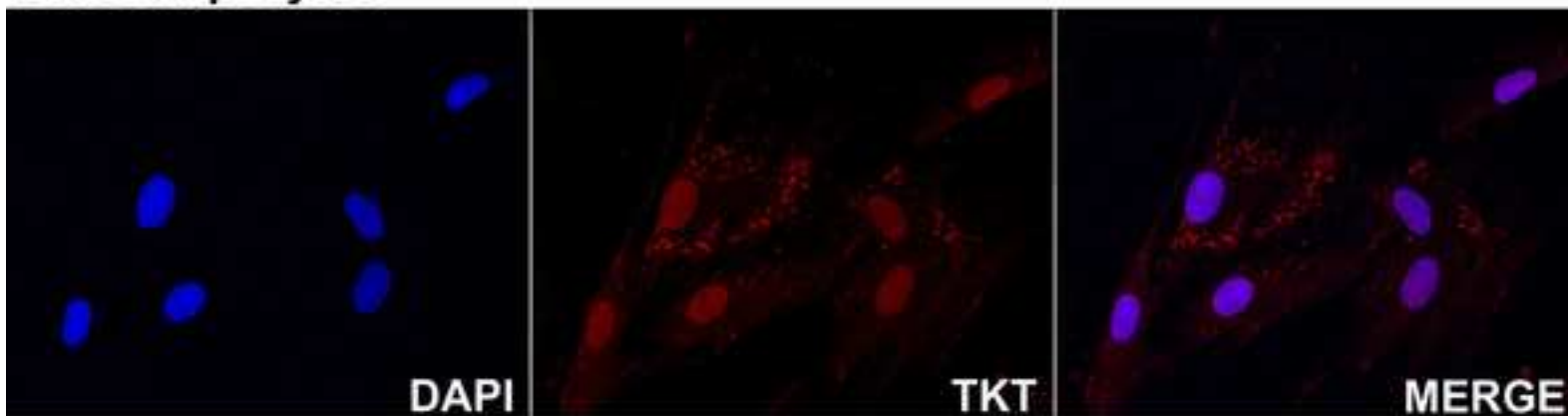


Fig4. Immunofluorescence staining of TKT  
[Click here to download high resolution image](#)

### A. Omental Adipose Tissue



### B. Preadipocytes



### C. Adipocytes

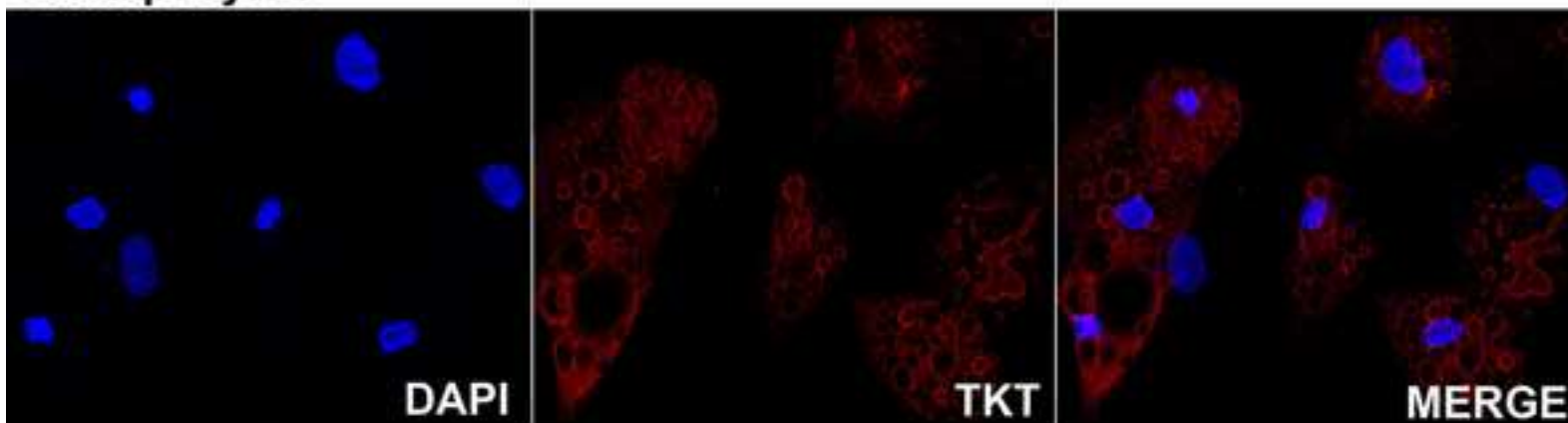
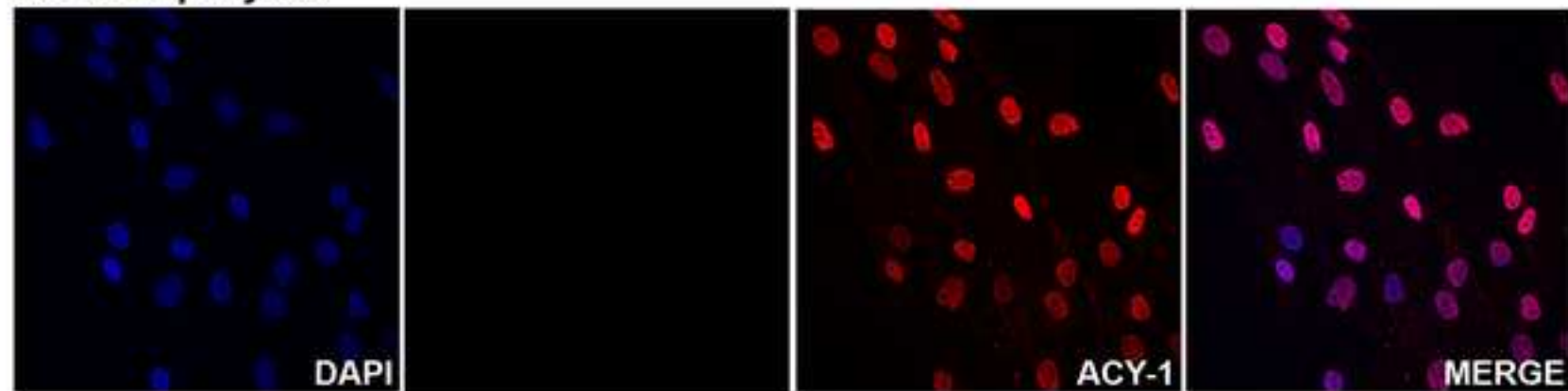
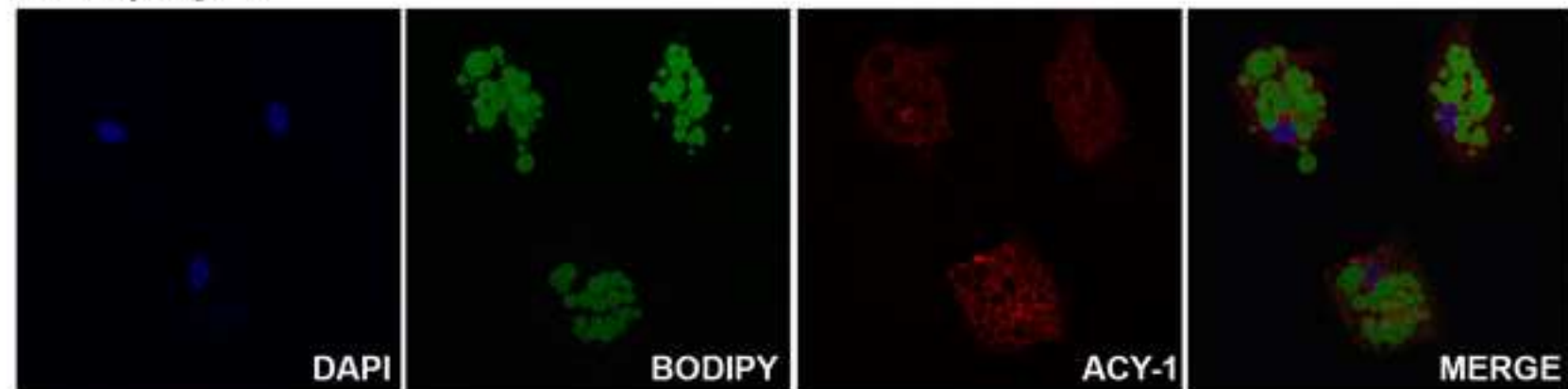


Fig5. Immunofluorescence staining of ACY-1  
[Click here to download high resolution image](#)

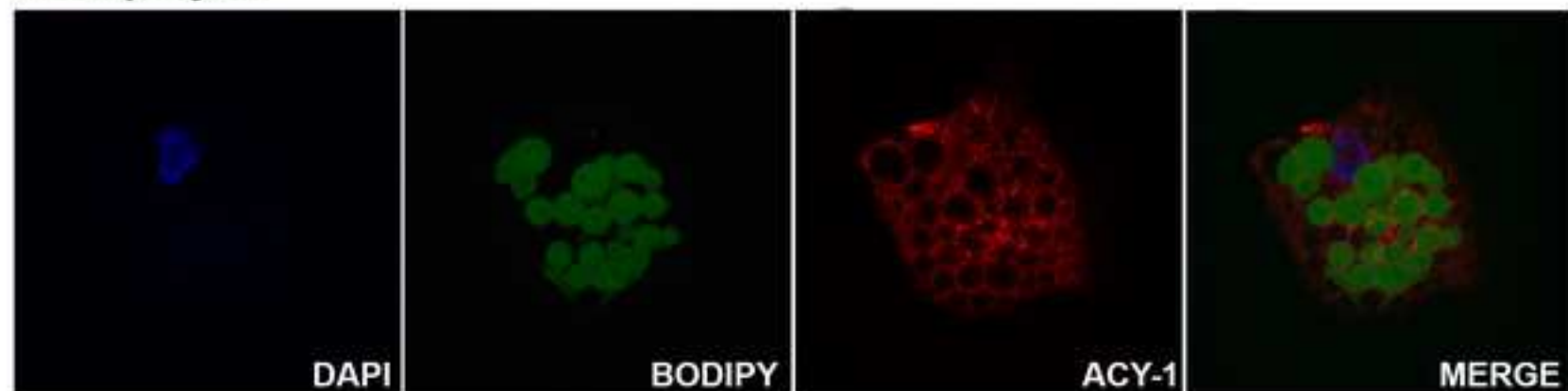
**A. Preadipocytes**

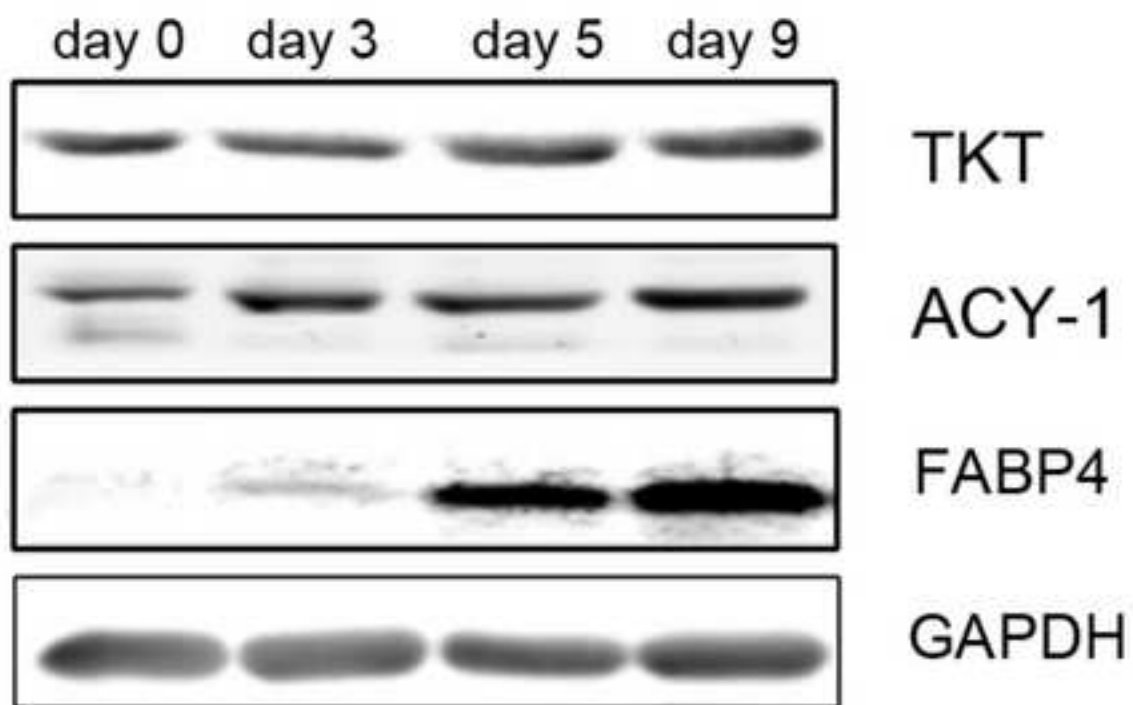
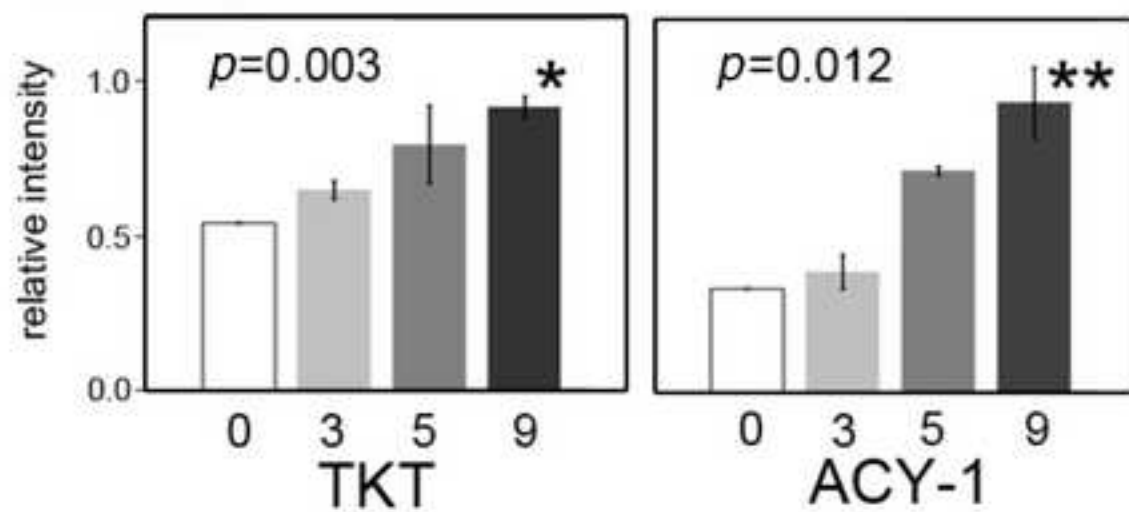


**B. Adipocytes**



**C. Adipocytes**



**A****B**



**Supplementary material**

[Click here to download Supplementary material: Supplementary Information.doc](#)

**Supplementary Table 1**

[Click here to download Supplementary material: Supplementary Table1.pdf](#)

**New Supplementary Table 2**

[Click here to download Supplementary material: Supplementary Table 2.pdf](#)